

# **Diagnostic Accuracy of Cone Beam Computed Tomography in Detection of Arthritic Changes of Rat's Temporomandibular joint Condyle in Correlation with Histological Findings**

## **Thesis**

Submitted to the Department of Oral Medicine, Periodontology, Oral  
Radiology and Diagnosis, Faculty of Dentistry, Ain Shams University, in  
Partial Fulfillment of the Requirements for Master Degree in  
**Oral Radiology and Diagnostic Sciences**

## **Presented by**

***SAHAR MOHAMED SAMIR MORSY***

B.D.S, Ain shams University (2007)

## **Supervised by**

**Dr.Mona Abou-el Fotouh**

Assistant Professor of Oral Radiology and Diagnostic Sciences  
Faculty of Dentistry  
Ain Shams University

**Dr. Walaa Mohamed Hamed**

Lecturer of Oral Radiology and Diagnostic Sciences  
Faculty of Dentistry  
Ain Shams University

**Faculty of Dentistry  
Ain Shams University**

**2013**

وَقُلْ رَبِّ زِنِّي عَلِمًا

طه ١١٤

# ACKNOWLEDGMENT

*All praise and gratitude be to ALLAH with the blessings of whom the good deeds are fulfilled.*

I wish to express my deep gratitude to **Dr. Mona Abou-El Fotouh**, for her encouragement, patience, and endless support throughout the research steps.

Also, I am greatly indebted to **Dr. Walaa Hamed**, for her valuable advices and suggestions. Her helpful comments and discussions during our meetings are greatly appreciated.

I would like to express my deepest appreciation to all members of *Oral Biology and Oral Pathology departments, Faculty of Dentistry, Ain Shams University* with special thanks to **Dr. Safaa Ismael**, for the great help in histologic sections of my work.

Also I am greatly indebted to *Drs: Mary Medhat, Hany El-Zohiery, Fatma El-badawy, Shaimaa Abo-Alsadat, Sara El-Khateeb*, and all faculty members of the *Oral Radiology department, Faculty of Dentistry, Ain Shams University* for their assistance in observations and for continued help and support.

Special thanks to the staff members of *Photon Imaging Center* and to all members of *Animal House of "the Medical Research Center" in Cairo University* for their help, support and flexibility during the practical part of this research. Also I would like to thank *Dr. Sherif Abd-Allah* for his assistance with the statistical analysis.

A great endless appreciation and thanks to my family, for their continuous support, encouragement, help and guidance.

*Sahar Samir*

---

# TABLE OF CONTENTS

Title	Page
Introduction and review of literature	1
Aim of the study	33
Materials and methods	34
Case presentation	52
Results	61
Discussion	78
Summary and conclusion	90
Recommendations	92
References	93
Arabic summary	--

---

---

# LIST OF TABLES

Table	Title	Page
<b>1</b>	Summary of scanning parameters and properties of CBCT machine ( <b>Planmeca ProMax3D Proface</b> )	<b>37</b>
<b>2</b>	Comparison between CBCT and histological observations of osseous changes	<b>62</b>
<b>3</b>	Diagnostic performance of CBCT observations	<b>64</b>
<b>4</b>	The intra-observer reliability of observer (1)	<b>65</b>
<b>5</b>	The intra-observer reliability of observer (2)	<b>67</b>
<b>6</b>	The inter-observer reliability of the 1 <sup>st</sup> readings	<b>96</b>
<b>7</b>	The inter-observer reliability of the 2 <sup>nd</sup> readings	<b>71</b>
<b>8</b>	Comparison between bone density values of study and control groups measured by histological analysis	<b>73</b>
<b>9</b>	Comparison between density value measurements of study and control groups measured by CBCT-VV	<b>75</b>
<b>10</b>	The correlation between bone density values measured by histological analysis and values measured by CBCT-VV	<b>77</b>

---

---

# LIST OF FIGURES

Figure	Title	Page
<b>1</b>	Autopsy specimen showing components of the human's TMJ; glenoid fossa (GF), articular eminence (AE) of the temporal bone (TB), mandibular condyle (MC), articular disc (AD) and synovial capsule (SC)	<b>2</b>
<b>2</b>	Normal histological section of human's TMJ	<b>2</b>
<b>3</b>	Lateral view of rat's skull and mandible showing prominent mandibular angle (blue arrow) and divergent condyles (yellow arrow)	<b>4</b>
<b>4</b>	Histological sections of rat's TMJ c= condyle, d= disc, t= temporal bone, rd= retro-discal tissue	<b>4</b>
<b>5</b>	Sagittal CBCT images showing different arthritic changes of the human condyle	<b>7</b>
<b>6</b>	MDCT images for the human's TMJ (a) Sagittal oblique soft-tissue window shows anterior disc displacement. (b) Sagittal oblique bone window shows condylar flattening, irregularity, sclerosis and small osteophyte	<b>10</b>
<b>7</b>	Different imaging modalities of the human mandibular condyle condyle (a): Corrected sagittal tomography (b): Helical CT (c): limited cone beam CT	<b>10</b>
<b>8</b>	CBCT imaging geometry	<b>12</b>
<b>9</b>	Different FOVs of CBCT	<b>13</b>
<b>10</b>	CBCT imaging using CsI detector	<b>16</b>
<b>11</b>	Isotropic voxel resolution of CBCT compared to anisotropic voxel of conventional CT	<b>16</b>

---

<b>12</b>	<b>Stages for volumetric data production in CBCT</b>	<b>18</b>
<b>13</b>	Standard display modes of CBCT volumetric data; A: Volumetric 3D representation. B: Axial image. C: Sagittal image, and D: Coronal image (Dolphin 3D, Chatsworth, California)	<b>20</b>
<b>14</b>	<b>Reconstruction of ray sum images by CBCT</b>	<b>20</b>
<b>15</b>	<b>Effective doses from various dental radiographic procedures</b>	<b>22</b>
<b>16</b>	<b>Schematic demonstration of methods for reducing x-ray scatter at the detector</b>	<b>24</b>
<b>17</b>	Exponential edge gradient effect of metallic crown with the typical thin lines tangent to sharp edges of metallic crowns (arrows) in the direction of the beam	<b>24</b>
<b>18</b>	<b>Pre and post surgical models and superimposition of them for maxillofacial surgical evaluation by CBCT software (Dolphin 3D imaging)</b>	<b>25</b>
<b>19</b>	<b>Fusion of CBCT data and photographic image for orthodontic planning (Next Generation i-CAT CBCT)</b>	<b>28</b>
<b>20</b>	<b>Linear measurements of the human mandibular condyle using CBCT software (NewTom Model QR-DVT 9000, Verona, Italy)</b>	<b>31</b>
<b>21</b>	<b>Volumetric assessment of degenerative osseous changes of human condyle using CBCT software (NewTom Model QR-DVT 9000, Verona, Italy)</b>	<b>31</b>
<b>22</b>	<b>CBCT examination of rat's mandible using ILUMA 3D software (Materialize, Glen Burnie, MD)</b>	<b>32</b>
<b>23</b>	<b>Injection of intra-peritoneal anesthesia</b>	<b>45</b>
<b>24</b>	<b>CFA injection. A-Showing Joint palpation before injection. B- Showing intra-articular injection of CFA</b>	<b>46</b>

	Stabilization of rat heads on CBCT machine. A: Showing rat	
<b>25</b>	heads supported by rubber base impression material. B: Showing CBCT machine <b>Planmeca ProMax3D Proface</b>	<b>46</b>
<b>26</b>	Multiplanar reformatted view using <b>Planmeca Romexis Viewer 3.0.0.R</b>	<b>47</b>
<b>27</b>	Showing orientation of sagittal line	<b>48</b>
<b>28</b>	Sequential sagittal slices. A: high contrast image. B: Low contrast image	<b>48</b>
<b>29</b>	Showing orientation of Coronal line	<b>49</b>
<b>30</b>	Coronal slice of CBCT. A: high contrast image. B: Low contrast image.	<b>49</b>
<b>31</b>	Orientation of axial line	<b>50</b>
<b>32</b>	Axial slice of CBCT. A: high contrast image. B: Low contrast image.	<b>50</b>
<b>33</b>	Determination of bone density value using CBCT	<b>51</b>
<b>34</b>	Sagittal H&E histological section of rat's TMJ	<b>51</b>
<b>35</b>	Histological image analysis of bone density A: Before subtraction of bone marrow and cartilaginous cap. B: Bone content after subtraction of bone marrow and cartilaginous cap	<b>51</b>
<b>36</b>	Coronal CBCT high contrast image showing normal rat's condyle with a regular mesiodistal outline	<b>52</b>
<b>37</b>	Axial CBCT high contrast image showing normal rat's joint space	<b>52</b>
<b>38</b>	Sagittal CBCT low contrast image showing normal rat's condyle with a regular anteroposterior outline	<b>53</b>

<b>39</b>	The CBCT voxel value of the normal rat's condyle measured at the sagittal slice	<b>53</b>
<b>40</b>	A sagittal H&E section showing normal rat's TMJ	<b>54</b>
<b>41</b>	Threshold adjustment of the condylar bone content for the same H&E section.	<b>54</b>
<b>42</b>	Coronal CBCT high contrast image showing increased mesiodistal dimension of the condyle	<b>55</b>
<b>43</b>	Axial CBCT low contrast image showing totally obliterated joint space	<b>55</b>
<b>44</b>	Sagittal CBCT low contrast image showing increased anteroposterior dimension of the condyle	<b>56</b>
<b>45</b>	Reduced CBCT voxel value of the condyle measured at the sagittal slice	<b>56</b>
<b>46</b>	A sagittal H&E section showing reduced joint space (a) with wide marrow spaces (b)	<b>57</b>
<b>47</b>	Threshold adjustment of the condylar bone content for the same H&E section.	<b>57</b>
<b>48</b>	Coronal CBCT high contrast image showing decreased mesiodistal dimension of the condyle due to erosion	<b>58</b>
<b>49</b>	Axial CBCT low contrast image showing no change of the joint space	<b>58</b>
<b>50</b>	Sagittal CBCT low contrast image showing irregular condylar surface due to erosion	<b>59</b>
<b>51</b>	Reduced CBCT voxel value of the condyle measured at the sagittal slice	<b>59</b>
<b>52</b>	A sagittal H&E section showing erosion of the condyle resulting in irregular surface (a) and wide marrow spaces (b)	<b>60</b>

<b>53</b>	Threshold adjustment of the condylar bone content for the same H&E section.	<b>60</b>
<b>54</b>	Column chart showing comparison between CBCT and histological observations of osseous changes	<b>63</b>
<b>55</b>	Column chart showing intra-observer reliability of the CBCT observer (1)	<b>66</b>
<b>56</b>	Column chart showing intra-observer reliability of the CBCT observer (2)	<b>68</b>
<b>57</b>	Column chart showing inter-observer reliability of the 1 <sup>st</sup> reading	<b>70</b>
<b>58</b>	Column chart showing inter-observer reliability of the 2 <sup>nd</sup> reading	<b>72</b>
<b>59</b>	Column chart showing comparison between bone density values of study and control groups measured by histological analysis	<b>74</b>
<b>60</b>	Column chart showing comparison between bone density values of study and control groups measured by CBCT-VV	<b>76</b>
<b>61</b>	Scatter plot showing correlation between CBCT-VV and histological bone density values	<b>77</b>

---

## LIST OF ABBREVIATIONS

Abbrev.	Full Term
<b>2D</b>	Two dimensional
<b>3D</b>	Three dimensional
<b>ACFT</b>	Axially Corrected Frontal Tomography
<b>ACST</b>	Axially Corrected Sagittal Tomography
<b>AIA</b>	Adjuvant induced arthritis
<b>a-Se</b>	Amorphous Selenium
<b>CBCT</b>	Cone Beam Computed Tomography
<b>CCD</b>	Charged Couple Device
<b>CFA</b>	Complete Freund's Adjuvant
<b>CsI</b>	Cesium Iodide
<b>CT</b>	Computed Tomography
<b>DICOM</b>	Digital imaging and Communication in Medicine
<b>EDTA</b>	Ethylene Diamine Tetra-acetic acid
<b>EEGE</b>	Exponential edge gradient effect
<b>FDK</b>	Feldkamp Algorithm

---

<b>FOV</b>	Field Of View
<b>FPD</b>	Flat Panel Detector
<b>H&amp;E</b>	Haematoxylin and Eosin
<b>HCT</b>	Helical CT
<b>HRUS</b>	High Resolution Ultrasound
<b>HU</b>	Hounsfield unit
<b>IID</b>	Image Intensifier Detector
<b>JIA</b>	Juvenile idiopathic arthritis
<b>MDCT</b>	Multi Detector CT
<b>MIP</b>	Maximum Intensity Projection
<b>MPR</b>	Multiplanar Reformatted
<b>MRI</b>	Magnetic Resonance Imaging
<b>NPV</b>	Negative predictive value
<b>OA</b>	Osteoarthritis
<b>OBS</b>	Observer
<b>PPV</b>	Positive Predictive value
<b>TFT</b>	Thin Film Transistor
<b>TMDs</b>	Temporomandibular Disorders
<b>TMJ</b>	Temporomandibular Joint
<b>VV</b>	Voxel Value

---

# **INTRODUCTION AND REVIEW OF LITERATURE**

Temporomandibular joint (TMJ) is one of the most complex joints in the human body. Its primary function is to facilitate mandibular movements, thus it plays a great role in mastication and speech. Joint movement is controlled by strong muscles and ligaments which guide its complex movements (*Ingawalé and Goswami, 2009*).

TMJ is a synovial joint formed by the mandibular condyle fitting into the glenoid fossa of the temporal bone. Condyle is the mobile portion during mandibular movements while the fossa remains stationary. Articular disc separates these two bones from direct contact and aids in the distribution of forces. The disc is attached to the condyle medially and laterally by collateral ligaments (*Laskin and Hylander, 2006*) **Fig (1)**.

Histologically, articulating surfaces are covered by fibrocartilage with a greater capacity to resist degenerative changes and regenerate itself more than the hyaline cartilage of other synovial joints (*Pertes and Gross, 1995 and Ingawalé and Goswami, 2009*). Dense fibrous connective tissue disc divides the joint cavity into upper and lower components. It has a thin central area while the anterior and posterior regions are thicker (*Toriya et al., 2006 and Shibukawa et al., 2007*) **Fig (2)**.

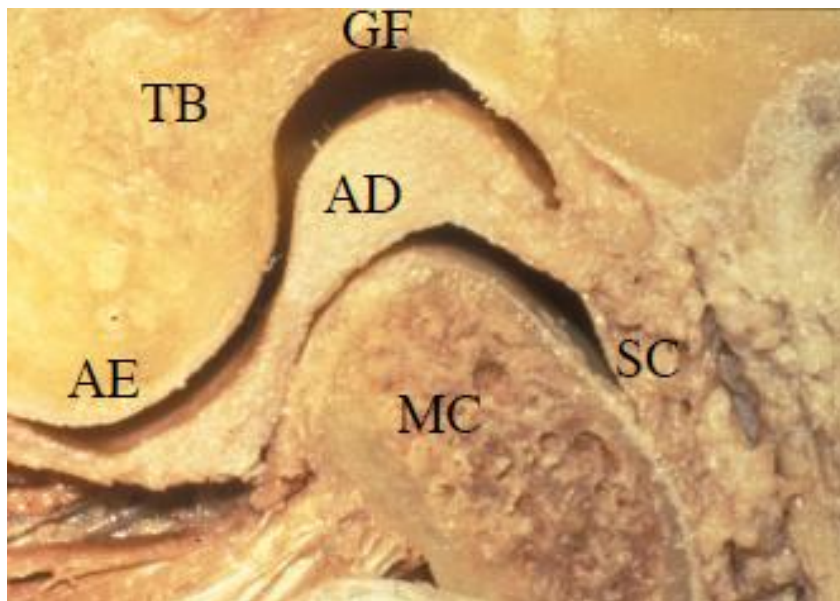


**Figure (1):** Autopsy specimen showing components of human's TMJ; glenoid fossa (GF), articular eminence (AE) of the temporal bone (TB), mandibular condyle (MC), articular disc (AD) and synovial capsule (SC) (*Wadhwa and Kapila, 2008*).

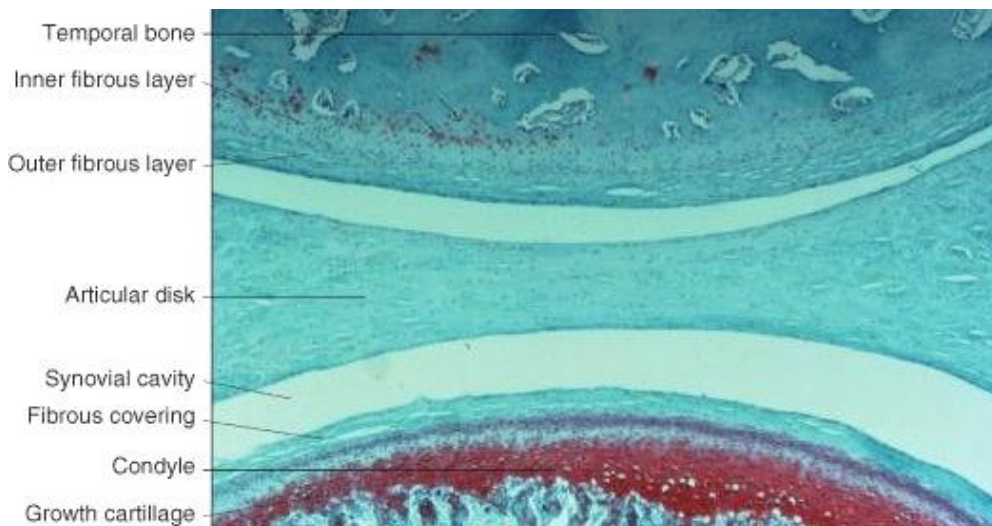


**Figure (2):** Showing normal histological section of human's TMJ (*Cate's and Nanci, 2008*).